Title: Pathogenic IgE-fated B cell memory retains functional plasticity

Authors: Kelly Bruton,[1†‡*], Allyssa Phelps,[1‡] Atai Ariaz[1], Tina D. Walker[1], Jianping Wen[1], Sharon S. Khavkine-Binstock[1], Allison Fang[1], Olivia Mann-Delany[1], Niels Peter H. Knudsen[2], Siyon Gadkar[1], Emily Grydziuszko[1], Joshua F. E. Koenig[1], Aidan Gagnon[1], Susan Waserman[1], Peter S. Andersen[2], Manel Jordana[1]

Affiliations:

[1]Schroeder Allergy & Immunology Research Institute and Department of Medicine (Division of Clinical Immunology & Allergy), McMaster University; Hamilton, Ontario, CA.

[2]ALK-Abelló A/S; Hørsholm, DK

[†]Current Address: Department of Pathology, Stanford University School of Medicine; Stanford, California, USA.

[‡]These authors contributed equally to this work.

*Corresponding author. Email: brutonk@stanford.edu

Abstract: Long-lived immunoglobulin (Ig) E responses against innocuous environmental and dietary antigens (Ags) are maintained by an IgG1-dominant memory B cell (MBC) compartment primed for IL-4 responsiveness. In this work, we investigated the plasticity of the MBC compartment fated for IgE class switch recombination upon Ag re-exposure. Antibody-mediated IL-4Rα blockade augmented the germinal center response and uncovered an IL-4/IL-13 dependency within the type 2 memory B cell (MBC2) skewed phenotype. In the absence of IL-4/IL-13 signaling during the recall response, a long-lived Ag-specific IgG2c MBC population emerged, shifting the MBC response away from a type 2 phenotype and towards type 1. The

emergence of this IgG2c response was dependent on IFN-γ signaling and arose from both unswitched and class-switched Ag-specific B cells *in vivo*. We further demonstrated that a type 1-polarizing adjuvant can augment the redirection of type 2-polarized class-switched MBCs, suggesting with the correct cues pathogenic MBCs can be functionally reprogrammed.

One Sentence Summary: B cell responses to allergens can be reprogrammed away from a pathogenic fate through IL-4/IL-13 signaling blockade.

Main Text:

INTRODUCTION

Classical immunological memory is marked by the propensity for rapid and optimized responses upon re-exposure to the target antigen (Ag). Within the B cell compartment, immunological memory is distinguished by high-affinity binding to Ag, a class-switched constant region conferring specialized effector functions, and altered cellular processes (*e.g.,* metabolism). Following vaccination, for example, viral exposure rapidly reactivates memory B cells (MBCs) facilitating plasma cell differentiation and boosting of neutralizing IgG titers, lessening the opportunity for infection (*1–3*). This same process, however, is pathogenic when perpetuating inflammatory responses to innocuous Ag, as occurs in allergic disease.

Allergies categorized as type I hypersensitivities are mediated by IgE. Humoral IgE responses are relatively short-lasting, yet reactivity to some allergens (*e.g.,* peanuts) can persist for a lifetime (*4–8*). Central to this persistence are IgG1^{+} MBCs which undergo sequential class-switching to replenish the transient IgE plasma cell pool (*5*, *9–11*). Likewise, it has been identified that IgE-fated MBCs, termed MBC2s, exhibit an IL-4-responsive phenotype marked by high expression of CD23 (FcεRII) and IL-4 receptor α (IL-4Rα) and low CD32 (FcγRII)

31 expression (*12–14*). Indeed, seminal work on IgE established IL-4 as a critical molecule for IgE
32 class switch recombination (CSR) upon primary sensitization (*15*, *16*). Despite the formation of a
33 more specialized MBC compartment, IL-4 continues to be required for secondary IgE responses
34 (*17–19*). Beyond inhibition of IgE CSR, loss of IL-4 signaling upregulates IFN-γ production
35 suggestive of plasticity within the T cell compartment (*17*). Whether a parallel degree of
36 plasticity exists in Ag-specific MBCs, or if the commitment is irreversible, remains to be
37 elucidated.

38 In this study, we identified a previously unrecognized plasticity of MBCs within type 2
39 immunity. By inhibiting IL-4 signaling in a recall response, the pathogenic MBC2 phenotype
40 was diminished and upregulation of IFN-γ supported the emergence of long-lived IgG2
41 responses. Even beyond transient IL-4Rα blockade, IgG2 reemerged upon Ag exposure,
42 suggesting some degree of stability in the type I-like reprogrammed Ab response despite
43 discontinued IL-4Rα blockade. Ag-specific IgG2 responses appeared to derive from both
44 unswitched B cells and class-switched MBCs, where the addition of a type 1 adjuvant could
45 augment the redirection of IgG1 memory to IgG2. Collectively, our findings elucidate a
46 malleable fate of pathogenic IgE-fated MBCs and highlights the potential to therapeutically
47 reprogram refractory lifelong allergies.

48 **RESULTS**

49 **IL-4Rα signaling augments secondary germinal center activity**

50 To assess the impact of *in vivo* anti-IL-4α (A4RA) treatment on the B cell compartment in type 2
51 immunity, we employed a well characterized model of epicutaneous sensitization to ovalbumin
52 (OVA). This strategy establishes a humoral OVA-IgG1 response and $IgG1^{+}$ MBCs which, upon

53 subsequent non-sensitizing subcutaneous (s.c.) re-exposures, facilitate IgE production and IgE-
54 mediated clinical reactivity (*20*). With temporal control over the IgE response, we treated
55 sensitized mice with A4RA or an isotype control (IC) prior to s.c. re-exposures, as previously
56 described (*17*). Draining lymph nodes (dLNs) and spleens were collected for single-cell RNA-
57 sequencing (scRNA-seq), single-cell VDJ-sequencing (scVDJ-seq), and flow cytometry, and
58 blood was collected for immunoglobulin (Ig) analysis (**Fig. 1A**). For scRNA- and scVDJ-seq
59 experiments an additional group of mice were administered cholera toxin (CT) and OVA (s.c.) to
60 model a classical type 2 immunization strategy that yields robust humoral IgE responses and
61 IgG1^{+} MBCs.

62 Four weeks following immunization and s.c. re-exposures, paired scRNA-seq and scVDJ-seq
63 were performed on 7,369 B cells. Clustering analysis revealed subsets of naïve B cells (*Ighm*$^{+}$
64 *Ighd*$^{+}$), class-switched MBCs (*Ighm*$^{-}$ *Ighd*$^{-}$), and an *Ighd*$^{+/-}$ subset defined by high *Fcrl5* and
65 *Apoe* expression (**Fig. 1B and 1C**). Naïve-1 was the dominant naïve subset in CT and IC-treated
66 mice, though was almost completely replaced by the Naïve-4 cluster in A4RA-treated mice (**Fig.
67 1D**). Naïve-4 cells exhibited marked transcriptional downregulation, particularly across several
68 metabolic pathways and genes relating to Ag presentation and cellular localization (**fig. S1A and
69 S1B**). Indeed, it has been shown that *in vitro* B cell stimulation with IL-4 initiates metabolic
70 reprogramming and MHC-II upregulation (*21–23*). The Naïve-3 subset, which was almost
71 exclusively found in epicutaneously sensitized mice, had upregulated *Il31ra* expression, the
72 ligand (IL-31) of which is implicated in promoting dermatitis (**fig. S1C and S1D**) (*24*). Other
73 naïve and MBC clusters were similarly represented between the three groups. Across all core
74 naïve clusters (1-5) and MBCs, A4RA treatment resulted in downregulated oxidative

75 phosphorylation and B cell receptor (BCR) signaling gene modules – two imperative processes
76 for germinal center (GC) activity (**Fig. 1E**) (*25*, *26*).

77 Previous reports have demonstrated a critical requirement of IL-4 signaling for primary GC
78 activity in models of type 2 immunity, though it remains unclear whether this requirement is
79 maintained for secondary responses where primary responses can prime MBCs for a GC or PC
80 fate (*27–29*). The requirement of secondary GC activity to mount an IgE response in
81 epicutaneously sensitized mice was confirmed using CD40L blockade before and during s.c. re-
82 exposures, whereby anti-CD40L prevented OVA-specific IgE production and clinical reactivity
83 (**fig. S2A-C**). To investigate how an IL-4/IL-13 signaling deficiency might impact secondary
84 GCs, we utilized the paired scRNA- and scVDJ-seq data to determine the extent of somatic
85 hypermutation (SHM) within the MBC cluster. Despite an absence of highly mutated sequences
86 with A4RA treatment, the overall extent of somatic hypermutation was not significantly different
87 between groups (**Fig. 1F**).

88 As the above findings provided only transcriptional insight within the bulk (non-Ag-specific) B
89 cell repertoire, we assessed the impact of A4RA on OVA-specific B cells by flow cytometry
90 using fluorochrome-conjugated OVA tetramers (*30*). In agreement with the altered B cell
91 metabolic profile in the transcriptomic data suggestive of compromised B cell survival and/or
92 proliferative capacity, the frequency of OVA^+ B cells was 3-fold lower in A4RA-treated mice,
93 with an average of 406 versus 1269 cells per dLN pair in A4RA and IC groups, respectively
94 (**Fig. 1G and 1H**). Expression of CD38 and GL7 identifies three populations of B cells differing
95 in their activation states: $CD38^+$ $GL7^-$ resting naïve/memory (1), $CD38^+$ $GL7^+$ transitional or
96 multipotent precursor cells (2), and $CD38^-$ $GL7^+$ GC B cells (3) (**Fig. 1I**) (*31*). At three days
97 post-re-exposures, the A4RA group had significantly impaired OVA-specific B cell activation,

98 evidenced by an increased frequency of CD38^{+} GL7^{-} OVA-specific B cells and a concomitant
99 decrease in the CD38^{-} GL7^{+} population (**Fig. 1J**). However, 23% of OVA-specific B cells in
100 A4RA-treated mice were in a transitional state compared to 2.6% in IC-treated mice, which
101 suggested that loss of IL-4/IL-13 signaling altered the kinetics of MBC reactivation. Indeed,
102 assessment of GC activity at 7-, 14-, and 28-days post-re-exposure demonstrated that the
103 magnitude of GC activity is no different between groups and A4RA treatment merely stalls early
104 GC formation (**Fig. 1K**). Taken together, these data suggest that loss of IL-4/IL-13 signaling
105 elicits profound transcriptional changes to naïve B cells and MBCs, but GC-dependent recall
106 responses can ultimately proceed.

107 **MBC2 phenotype is ameliorated with IL-4Rα blockade in mice and humans**

108 MBC2s have been identified as an important reservoir for pathological IgE responses.
109 Previously, IL-4 was shown to be necessary for MBC2 development and, likewise, blockade of
110 IL-4/IL-13 signaling issued a decline in MBC2 frequency (*12*, *13*, *17*). Despite the observed
111 decrease in MBC2s a small number persist, though whether expression of the pathogenic IL-4-
112 responsive phenotype is maintained to the same extent has not been explored.

113 To address this, we leveraged publicly reposited B cell scRNA-seq datasets involving
114 perturbation of IL-4/IL-13 signaling. Including our own data generated above, our analysis
115 involved four data sets comprising both mouse and human, various models of type 2 immunity,
116 enhanced and abrogated IL-4/IL-13 signaling, and with or without Ag re-exposure (**Fig. 2A**) (*17*,
117 *32*, *33*). For each dataset, unsupervised clustering was performed on B cells (*Cd79a*$^{+}$), which
118 resolved clusters of MBCs classified by absence of *Ighd*, *Tcl1a* (human), and *Bcl6* (mouse) and
119 the presence of *Hhex* (mouse) expression (**Fig. 2B and S3A-D**). *Fcer2*, *Il4r*, and *Ighg1*
120 expression was compared between each control and interventional group to evaluate the impact

121 of enhanced or inhibited IL-4/IL-13 signaling on MBC2-related gene expression (**Fig. 2C**).
122 *Fcer2* expression in MBCs was consistently downregulated across datasets involving IL-4/IL-13
123 signaling inhibition. IL-4Rα blockade also elicited a decline in *Il4r* expression, apart from
124 epicutaneously sensitized mice where *Il4r* transcript abundance was also low in IC mice.
125 Conversely, with increased IL-4/IL-13 bioavailability to B cells through elimination of its uptake
126 by lymphoid stromal cells (*Ccl19*$^{Cre/+}$ *Il4ra*$^{fl/fl}$ bone marrow chimeras), *Fcer2* and *Il4r* expression
127 was enhanced within the MBC cluster (*32*). Intriguingly, *Ighg1* expression was downregulated
128 only in experimental systems involving Ag re-exposure during IL-4Rα blockade.

129 To corroborate the diminished MBC2 phenotype within Ag-specific cells, we assessed co-
130 expression of surface IL-4Rα and CD23 on tetramer^{+} MBCs by flow cytometry four weeks
131 following *s.c.* re-exposures in epicutaneously sensitized mice (**Fig. 2D**). A4RA-treated mice
132 exhibited a 61% reduction in the frequency of IL-4Rα^{+} CD23^{+} cells in the OVA-specific MBC
133 compartment (**Fig. 2E**). Loss of IL-4Rα expression was not an artifact of impaired detection due
134 to the *in vivo* blocking antibody as there was no increase in the frequency of CD23 single-
135 positive cells (**Fig. 2E**). Consistent with a role of IL-4 in inducing CD23 expression, A4RA
136 treatment decreased surface expression of CD23 (**Fig. 2F**) (*34*). CD23 downregulation was not,
137 however, unique to Ag-specific cells, but instead was broadly observed throughout non-specific
138 MBCs (**Fig. 2F**).

139 To also validate the human scRNA-seq observations, we stimulated peripheral blood
140 mononuclear cells (PBMCs) from peanut-allergic donors (*n*=3) with crude peanut extract for 8
141 days in the presence or absence of A4RA. CD23^{+} IL-4Rα^{+} class-switched B cells were observed
142 in stimulated cells but were virtually undetectable with A4RA treatment (**Fig. 2G**). Consistent
143 with previous reports, CD23^{+} IL-4Rα^{+} cells had variable CD27 expression, though both

144 populations were similarly impacted by A4RA (**Fig. 2H**) (*12*, *13*). Moreover, as was observed in
145 mice, A4RA broadly decreased CD23 mean fluorescence intensity (MFI) within class-switched
146 B cells (**Fig. 2I**). Collectively, these data demonstrate a conserved requirement for IL-4/IL-13
147 signaling to maintain heightened type 2 polarization within established MBC compartments,
148 which contests a previous suggestion regarding MBC2 phenotypic resiliency (*12*). These data
149 also raise the issue of how Ag re-exposure during IL-4Rα blockade may skew the isotype
150 distribution away from IgG1 – the dominant intermediary for IgE CSR.

151 **Long-lived Ag-specific IgG2 responses emerge in the absence of IL-4/IL-13 signaling**

152 As we observed that recall responses occurred in the absence of IL-4/IL-13 signaling, alongside
153 dampened MBC2 polarization (including *Ighg1*) and prevented IgE CSR, we sought to define the
154 Ig product of recall responses. Evaluating isotypes downstream to IgG1 – the dominant memory
155 reservoir in epicutaneously sensitized mice – an increase in *Ighg2b* and *Ighg2c*, but not *Igha*,
156 transcripts was observed in the MBC cluster of A4RA-treated mice (**Fig. 3A**). From the paired
157 scVDJ-seq analysis we plotted the assigned *Ighc* gene for each MBC with at least three
158 nucleotide mutations (**Fig. 3B**). Consistent with the notion that IgE^+ MBCs are non-existent in
159 mice, *Ighe* sequences were undetected (*35*, *36*). The distribution of isotype usage was
160 comparable between CT and IC mice, except for *Ighg2b*, which had a substantially greater
161 presence in CT in agreement with the reported CT-induced secretion of TGF-β, a driver of
162 IgG2b CSR (*37*, *38*). By contrast, A4RA induced a pronounced increase in *Ighg2c* above both
163 CT and IC – an isotype that is not associated with type 2 immunity.

164 To assess whether the skewed isotype usage occurred within the Ag-specific B cell repertoire
165 and the longevity of such response, OVA^+ MBCs and the OVA-specific serum Ig profile were
166 interrogated up to 15 weeks after the recall response. OVA^+ $IgG1^+$ MBCs were present in both

167 IC and A4RA-treated mice, though with a significantly decreased frequency with A4RA
168 treatment (**Fig. 3C and 3D**). By comparison, OVA$^+$ IgG2c$^+$ MBCs emerged with A4RA
169 treatment and were sustained beyond three months. The emergence of OVA$^+$ IgG2c$^+$ MBCs was
170 halted with concurrent IFN-γ receptor 1 blockade (**Fig. 3E**). This coincides with IgG2c CSR
171 being driven by IFN-γ and our previous work demonstrating an increase in IFN-γ production
172 with A4RA treatment (*17*, *39*, *40*). Skewed isotype usage was also reflected in the analysis of
173 serum OVA-specific Igs (**Fig. 3F**). As per our previous observations, serum OVA-IgE responses
174 were short-lived in IC mice with a completely abrogated response in A4RA-treated mice (*17*,
175 *20*). Consistent with the induction of IgG2c$^+$ MBCs, serum OVA-IgG2c was observed with
176 A4RA treatment though was not long-lived and declined at a similar rate to IgE in IC mice.
177 Disparate to the reduction in OVA$^+$ IgG1$^+$ MBCs, Ag re-exposure induced a comparable
178 resurgence of serum OVA-IgG1 in both groups, suggesting that A4RA may have limited impact
179 on MBCs fated for PC differentiation. Serum OVA-IgG2b titers were comparable between both
180 groups and OVA-IgA was undetectable.

181 We reasoned that if the skewed isotype response by A4RA was stably maintained then a
182 resurgence of IgG2c should be facilitated by seeded IgG2c$^+$ MBCs. To this end, mice were
183 provided tertiary OVA re-exposures nine weeks post-A4RA/IC and s.c. OVA administration. At
184 this point there is clearance of both serum OVA-IgG2c and the blocking A4RA antibody (*17*).
185 Indeed, tertiary Ag re-exposure provided a significant regeneration of OVA-IgG2b and OVA-
186 IgG2c though abrogation of OVA-IgE production remained (**Fig. 3G**). Collectively, these data
187 demonstrate that induction of a recall response with IL-4Rα blockade permit the emergence of a
188 non-type 2 antibody response and propose that this reprogrammed B cell response may be
189 maintained even following A4RA clearance.

190 LNs at distinct anatomical sites have been shown to differ in their predisposition to promote
191 inflammatory or tolerogenic responses towards Ags (*41*). In this regard, we also investigated
192 A4RA-induced isotype skewing in the context of oral immunization, which preferentially issues
193 tolerogenic IgA-dominant responses. As previously shown, one intragastric administration of Ag
194 + CT does not issue a humoral response (*42*, *43*), though Ag-specific Igs arise after subsequent
195 oral administration of Ag alone (*42*). We adopted this framework to provide systemic
196 administration of IC or A4RA prior to each oral Ag re-exposure (**fig. S4A**). Expectedly, IC-
197 treated mice exhibited a classical type 2 response marked by OVA^+ $IgG1^+$ MBCs in gut dLNs
198 and serum OVA-IgG1 and -IgE (**fig. S4B and C**). Mirroring observations from epicutaneous
199 sensitization, A4RA elicited the emergence of OVA^+ $IgG2c^+$ MBCs and serum OVA-IgG2b and
200 -IgG2c, while preventing OVA-IgE synthesis. Conversely, OVA re-exposures did initiate an IgA
201 response which was abrogated with A4RA, reconciling the requirement of IL-4 signaling for
202 mucosal IgA responses (*44*) (**fig. S4C**). Thus, loss of IL-4/IL-13 signaling during Ag re-exposure
203 preferentially promotes IgG2 responses irrespective of tissue site.

204 **Class switch origins of $IgG2^+$ clones are comprised of multiple isotypes**

205 The observed loss of MBC2 polarization and divergence towards non-IgE humoral response
206 indicate the potential to reprogram pathogenic IgE responses; however, it remains unclear
207 whether skewed isotype usage arises *de novo* (i.e., from naïve or unswitched B cells) or from
208 direct reprogramming of existing class-switched MBCs. To address this, we performed bulk VDJ
209 sequencing on the OVA-enriched B cell fraction from pooled LNs and spleens. Parallel analyses
210 with Ig sequences derived in the 10X dataset were carried out to gain insight as to whether the
211 effects of A4RA are occurring broadly throughout all B cells or are contained within the Ag-
212 specific repertoire. We found that IL-4/IL-13 signaling did not influence CDR3 length or SHM

213 in unswitched and class-switched B cell repertoires (**fig. S5A-D**); Apparent biases in V gene
214 usage were observed within the class-switched repertoire of OVA-enriched B cells (**fig. S5E**);
215 however, this was also observed within polyclonal B cells and thus is unlikely related to the
216 OVA-specific recall response (**fig. S5F**).

217 Broadly probing whether unswitched or class-switched cells were putative precursors to IgG2
218 clones, we first measured the correlation of paired IGHV and IGHJ gene usage between isotypes.
219 Expectedly, paired IGHV-IGHJ gene usage was most highly correlated between *Ighm* and *Ighd*
220 clones in both groups (**Fig. 4A**). IGHV-IGHJ gene usage in *Ighg2* clones also correlated most
221 strongly with *Ighm* and *Ighd* clones, though overlap with *Ighg3* and *Ighg1* clones was increased
222 in A4RA (correlation coefficient = 0.31 *Ighg3* and 0.34 *Ighg1*) compared to IC (correlation
223 coefficient = 0.14 *Ighg3* and 0.22 *Ighg1*). Next, we partitioned sequences into clonal lineages
224 through hierarchical clustering, as described previously (*45*, *46*). Consistent with the correlation
225 of V-J gene and isotype usage, the majority of clones related to IgG1 and IgG2 sequences were
226 IgD or IgM. The isotype distribution of other shared IgG1 and IgG2 clones was similar between
227 IC and A4RA (**Fig. 4B**), suggesting that loss of IL-4/IL-13 signaling did not influence the class
228 switch origins of IgG2. Accordingly, mutated IgG2 sequences were present in B cell lineage
229 trees containing expanded IgM, IgG3, and IgG1 clones, demonstrating that both naïve and class-
230 switched cells can give rise to IgG2 (**Fig. 4C**).

231 While IL-4/IL-13 signaling did not appear to influence isotype origins of IgG2, we reasoned that
232 an increased propensity for IgG2 class switching would be reflected in the transcriptome of Ag-
233 specific B cells. To this end, we performed Smart-Seq2 on OVA-specific cells yielding the
234 reconstruction of full length BCRs for 40 and 41 OVA^+ B cells from IC- and A4RA-treated
235 mice, respectively. Of the sequenced cells, 22 were class-switched, where *Ighg2b* (n = 2) and

236 *Ighg2c* (*n* =1) sequences were only present in the A4RA group, consistent with upregulated
237 *Ighg2b* and *Ighg2c* expression in the 10X dataset (**table. S2 and Fig. 3A and B**). The limited
238 throughput of this approach did not permit the detection of clonally related sequences within
239 either group. Comparing gene expression of unswitched cells, A4RA upregulated genes relating
240 to IFN-γ signaling, including *Ifitm2, Cd63, Ifi203,* and *Mars*; conversely, *Ptpn2*, a negative
241 regulator of IFN-γ signaling was downregulated, collectively supporting an altered disposition of
242 unswitched B cells to undergo IgG2 CSR (**Fig. 4D**). Likewise, A4RA *Ighg1*$^+$ OVA-specific B
243 cells upregulated some IFN-γ-related genes (*Ifitm2, Cd63, Ets1,* and *Jak1*), which were similarly
244 expressed in *Ighg2b/c*$^+$ cells (**Fig. 4E**). Taken together, blockade of IL-4/IL-13 signaling can
245 influence the transcriptional profile of both unswitched and class-switched OVA-specific B cells
246 to give rise to IgG2 responses *in vivo.*

247 **Type 1-polarizing adjuvant can redirect isotypic fate of type 2-polarized class-switched**
248 **MBCs**

249 Having demonstrated evidence that IgG3 and IgG1 – though infrequently – can be an
250 intermediate to an IgG2 isotype we next assessed whether the addition of a type 1-polarizing
251 adjuvant could augment the redirection of class-switched MBCs to IgG2b/c. We utilized an
252 adjuvanted re-exposure system to assess whether the type 1 adjuvant, CpG, can divert the Ag-
253 specific response of class-switched MBCs from type 2 immunized mice (**Fig. 5A**). Class-
254 switched OVA-enriched MBCs were sorted from OVA + Alum-immunized CD45.1$^+$ donor mice
255 and were transferred to B cell-deficient (muMT) CD45.2$^+$ naïve mice. Recipient mice were then
256 immunized with either OVA + CT or OVA + CpG. Of note, OVA + Alum immunization yields
257 an IgG1 and IgE dominant response, where over 85% of our transferred class-switched MBC
258 pool was IgG1$^+$ and less than 4% were IgG2b/c$^+$ (*47*) (**Fig. 5B**). Thus, any emergence of OVA-

259 IgG2 responses in recipient mice is not likely to represent an expansion of donor IgG2 clones.
260 Moreover, OVA + CT immunization produces more OVA$^+$ IgG2b/c$^+$ MBCs than Alum;
261 therefore, if any IgG2 clones in the donor pool do contribute to the OVA-IgG2 response in
262 recipients, we would expect to observe this with both CT and CpG immunization (**Fig. 5B**).

263 One week following adoptive transfer and immunization, donor (CD45.1$^+$) OVA$^+$ B cells and
264 OVA-specific Igs were detected in recipient mice. As anticipated, immunization of recipient
265 mice with OVA + CT drove emergence of OVA$^+$ IgG1$^+$ MBCs and serum OVA-IgG1 and -IgE.
266 In contrast, OVA$^+$ IgG2c$^+$ MBCs and serum OVA-IgG2b and -IgG2c became present in recipient
267 mice immunized with OVA + CpG, with a sustained absence of OVA-IgE (**Fig. 5C and 5D**).
268 Collectively, these data support that Ag re-exposure in the presence of a type 1 adjuvant can
269 redirect the fate of class-switched MBCs established under type 2-polarizing conditions.

270 **DISCUSSION**

271 MBCs, compared to naïve counterparts, acquire enhanced functional and metabolic properties
272 increasing fitness for recall responses to the same Ag. The MBCs established upon allergic
273 sensitization gain a unique propensity to switch to IgE upon subsequent allergen exposures,
274 under the influence of IL-4. Whether this specialized B cell memory is functionally plastic was
275 not yet established. Assessing transcriptional profile, BCR repertoire, Ag-specific cellular
276 memory, and humoral Ab responses, our work identifies the capacity to reprogram the
277 pathogenic IgE-fated response towards a type 1-like, non-pathogenic IgG2 program.

278 Numerous studies in mice and humans have now established that IgG1 is the dominant MBC
279 reservoir for IgE (*5*, *10*, *11*, *20*, *48*). Recent work by us and others have extended upon this
280 concept illustrating that IgE-fated MBCs ("MBC2s") express ε germline transcripts and
281 upregulate surface expression of CD23 and IL-4Rα, seemingly remaining prepared for IL-4

282 responsiveness (*12–14*). In the absence of IL-4/IL-13 signaling in a recall response, we have
283 previously shown that IgE responses are indeed averted, and cytokine production skews toward a
284 Th1 profile (*17*). In the present work investigating how IL-4Rα blockade impacts the B cell
285 repertoire beyond avoidance of IgE production, we found that loss of IL-4/IL-13 signaling *in*
286 *vivo* broadly suppresses gene expression, particularly relating to metabolic processes and BCR
287 signaling. Intriguingly, Ag re-exposure could still elicit Ag-specific GC activity in the absence of
288 IL-4/IL-13, an issue which has remained contentious (*27*, *49*, *50*).

289 As a primary product of a GC response is PC production, we were particularly intrigued to see a
290 sustained absence of serum IgE without a compensatory increase in IgG1. Coinciding with our
291 previous observations of an increased IFN-γ to IL-4 ratio, we found that A4RA treatment
292 induced an IFN-γ-dependent Ag-specific IgG2c response, which was otherwise absent with IC.
293 IgG2 antibodies, unlike IgG1, only weakly bind Fcγ receptors and thus, can regulate the pro-
294 inflammatory effector functions of IgG1 through competition for Ag binding (*51*, *52*). IgG2 is
295 postulated to also regulate IgE effector functions directly through engagement with an inhibitory
296 receptor, CD32b, on mast cells and basophils (*53*). Indeed, allergen desensitization is associated
297 with increases in allergen-specific IgG2, paralleling the well documented increases in IgG4 (*54–*
298 *56*). In our studies we found that serum titers of Ag-specific IgG2c were short-lived, however
299 tertiary Ag exposure could re-boost serum IgG2 titers without any observed increase in IgE.
300 Notably, the boosted IgG2 response occurred in the absence of continued IL-4Rα blockade
301 illustrating a sustained reprogramming of the Ag-specific B cell response.

302 The molecular cues which sustain the MBC2 phenotype have not yet been described. In the T
303 cell compartment, a subset of T helper cells, termed "Th2A" is uniquely associated with allergic
304 disease, much like the novel MBC2 subset (*57*). Th2A cells exhibit heightened Th2-like

305 properties and are terminally differentiated, persisting even with IL-4Rα blockade (*17*, *57*, *58*).
306 Here, we demonstrate that unlike Th2A cells, MBC2s do not harbor a refractory pathogenic
307 phenotype. This requirement of IL-4 to sustain heightened CD23 and IL-4Rα expression was
308 consistent amongst mouse models and humans and reaffirms early observations of IL-4-
309 regulated expression in bulk B cell populations (*34*, *59*). Interestingly, CD23 purportedly
310 augments allergen-specific responses through IgE-facilitated Ag-presentation (*60*, *61*). Thus, it is
311 plausible that depressed CD23 expression observed not only on MBC2s, but throughout the B
312 cell compartment, may curtail reactivation of allergen-specific CD4 T cells, though this remains
313 an area for future investigation.

314 Our analysis of BCR sequences revealed clonal relationships between IgG2 and all upstream
315 isotypes, including IgM/D, IgG3, and IgG1. These data, therefore, suggest that both naïve and
316 Ag-experienced B cells can contribute to the A4RA-induced IgG2 response. Indeed, we showed
317 functionally that the adoptive transfer of class-switched MBCs (composed of over 85% $IgG1^{+}$
318 cells) from type 2 immunized mice could issue IgG2 responses following a boost with a type 1-
319 polarizing adjuvant. Sequential CSR has been most extensively studied in the IgM to IgE
320 trajectory, where IgG1 is a dominant intermediary. Interestingly, over 50% of the bulk IgG2
321 repertoire in humans also arises through sequential CSR with an IgG1 intermediary (*62*). This is
322 somewhat surprising given that sequential rounds of V(D)J recombination are likely more
323 metabolically taxing to the host. One explanation for this could be that sequential, rather than
324 direct, CSR provides a means to regulate pro-inflammatory antibody-mediated effector
325 functions. In agreement, both vaccination and allergy yield IgG1 dominant responses, though
326 with chronic Ag exposure through repeated vaccination or allergen immunotherapy, a shift to the
327 "anti-inflammatory" isotype, IgG4, is observed (*55*, *63–66*). Here, we demonstrated that Ag

328 exposure in the absence in IL-4/IL-13 signaling could produce a similar effect – a deviation from
329 the IgG1-IgE axis to an IgG2 response. As IgG2 is uninvolved in allergic inflammation in both
330 mice and humans, this shift to allergen-specific IgG2 production could be considered "anti-
331 inflammatory". Nevertheless, clonal relationships between IgG2 and downstream IgE have been
332 reported (*9*); whether the induced $IgG2^+$ MBCs can later revert to a pathogenic IgE fate in
333 humans is yet to be studied.

334 In summary, our research demonstrates that IL-4/IL-13 signaling is required to sustain the IgE
335 fate of B cell responses in established allergic disease and that loss of IL-4/IL-13 signaling can
336 transform the allergen response to an innocuous type 1 phenotype. This not only bolsters the
337 applicability of anti-IL-4Rα as a novel therapeutic in food allergy, but also broadly illuminates
338 the potential to reprogram deviant B cell responses. Thus, further research is warranted to
339 establish the intrinsic determinants that govern MBC fate, which will be imperative in the
340 development of therapeutic strategies to correct deviant B cell responses in settings like allergy,
341 autoimmunity, and transplantation.

342 **MATERIALS AND METHODS**

343 **Mice**

344 Female C57BL/6 mice (6-8 weeks old) were purchased from Charles River Laboratories
345 (Wilmington, MA). Female B6.129S2-*Ighm*^{tmCgn} and B6.SJL-*Ptprc*^{a} *Pepc*^{b}/Boy mice (6-8 weeks
346 old) were purchased from Jackson Laboratories (Bar Harbor, ME). All experimentation was in
347 compliance with the McMaster University Research Ethics Board.

348 **Immunizations**

349 *Epicutaneous sensitization:* Epicutaneous sensitization to ovalbumin (Sigma-Aldrich, St. Louis,
350 MO) was conducted as previously described (*20*). For recall responses, three low-back
351 subcutaneous injections of 100 μg OVA were given over the course of a week. *Gastric*
352 *sensitization:* Mice received one intragastric gavage of 1 mg OVA with 5 μg cholera toxin (CT)
353 in PBS. Four weeks later, mice received 1 mg OVA in PBS weekly for three weeks via gavage.
354 *Subcutaneous sensitization:* Mice were immunized subcutaneously with 250 μg OVA and 5 μg
355 CT. *Intraperitoneal sensitization:* Mice were immunized intraperitoneally with 250 μg OVA and
356 250 μL Alhydrogel 2% (aluminum hydroxide [alum], InvivoGen, San Diego, CA), 40 μg CpG,
357 or 5 μg CT.

358 Serum for analysis of OVA-specific antibodies was collected through retro-orbital bleeding. For
359 allergen challenges, 5 mg OVA was intraperitoneally injected. Core body temperature and
360 clinical signs were recorded, as previously described, and hematocrit was measured at 40
361 minutes (*67*).

362 **Antibody Administration**

363 Anti-CD40L (MR-1), anti-IFNγ-R1 (GR-20), and anti-trinitrophenol IgG2a isotype control
364 (2A3) were purchased from Bio X Cell (Lebanon, NH). Anti-IL-4Rα (M1) was produced in-
365 house, as previously described (*17*). Original hybridomas were generated by Immunex
366 Corporation (Amgen, Thousand Oaks, CA) and were generously provided by Dr. Fred
367 Finkelman (University of Cincinnati).

368 One mg of anti-IL-4Rα, anti-IFNγ-R1, or isotype control was intraperitoneally injected the day
369 prior to s.c. re-exposures. Anti-CD40L (0.35 mg) or isotype control was intraperitoneally
370 injected on days -1, 0, and 2 of s.c. re-exposures.

371 **Tetramer Staining and Enrichment**

372 Purified OVA (Sigma-Aldrich, St. Louis, MO) was biotinylated (ThermoFisher Scientific,
373 Waltham, MA) and tetramerized with streptavidin-PE or streptavidin-APC (Agilent, Santa Clara,
374 CA), as previously described (*30*). For decoy tetramer, β-lactoglobulin (Sigma-Aldrich, St.
375 Louis, MO) was biotinylated. Streptavidin-PE or -APC was conjugated with DyLight 594 or
376 DyLight 755 esters (ThermoFisher Scientific) and was used to tetramerize the biotinylated- β-
377 lactoglobulin.

378 Cell pellets were resuspended and stained with 5 nM decoy tetramer in 20 μL FACS buffer (10%
379 FBS and 1 μM EDTA in PBS) and 2% rat serum for five minutes on ice. Five nM OVA tetramer
380 was added and incubation continued for 30 minutes. Cells were washed to remove unbound
381 tetramer and were incubated with anti-PE or -APC microbeads (Miltenyi Biotec, Germany) for
382 15 minutes on ice. Cells were passed through LS columns affixed to MACS magnetic separator
383 (Miltenyi Biotec). Bound fractions were eluted with FACS buffer.

384 For CD45.1 enrichments, cell pellets were resuspended in 20 μL FACS buffer with 0.25 μg
385 FcBlock (BioLegend) for five minutes on ice, then stained with anti-CD45.1-APC (A20;
386 BioLegend) for 30 minutes. Enrichment with anti-APC microbeads proceeded as described
387 above.

388 **Patient Samples**

389 A cohort of three peanut allergic donors, aged 9-23, were recruited to donate blood from
390 McMaster Children's Hospital and Hamilton Health Sciences (Hamilton, Ontario, Canada).
391 Allergic status was confirmed by peanut-specific IgE (higher than 0.35 kU/L) ImmunoCap at
392 Laboratory Reference Centre Hamilton (McMaster Children's Hospital). Donors were excluded

393 from the study for previous or current allergen immunotherapy, omalizumab, dupilumab or other
394 systemic immunomodulatory treatment, as well as diagnosed autoimmune or immunodeficiency
395 diseases. All donors were recruited with written consent and ethical approval from the Hamilton
396 Integrated Research Ethics Board.

397 Peripheral blood was collected into heparinized tubes (BD). PBMCs were isolated via Ficoll-
398 Paque (GE Healthcare) density centrifugation and were cryopreserved in FBS + 10% DMSO for
399 long-term storage in liquid nitrogen. Before culture, viability of thawed PBMCs was confirmed
400 to be ≥ 70%. PBMCs were cultured for 8 days and stimulated with 2.5 ng/mL crude peanut
401 extract (Stallergenes Greer) with or without 50 ug/mL anti-human IL-4Ra (R&D Systems), as
402 previously described (*17*).

403 **Flow Cytometry and Cell Sorting**

404 Single-cell suspensions were plated in U-bottom 96-well plates and incubated with 0.25 µg
405 FcBlock for 10 minutes on ice. Cells were stained extracellularly for 30 minutes on ice with
406 antibody cocktails prepared in FACS buffer. For intracellular staining, cells were fixed and
407 permeabilized with Cytofix/Cytoperm (BD Biosciences), as per manufacturer's instructions.
408 Intracellular antibody cocktails were prepared in 1x perm wash and cells were stained for 30
409 minutes on ice.

410 The following anti-mouse fluorochrome-conjugated antibodies were used: B220-AF700 (RA3-
411 6B2), CD138-PE/Dazzle 594 (281-2), CD3-BV711 (17A2), CD3-BV510 (17A2), F4/80-BV711
412 (BM8), F4/80-BV510 (BM8), CD38-PE/Cy7 (90), GL7-PerCP.Cy5.5 (GL7), GL7-BV421 (GL7;
413 BD, Franklin Lakes, NJ), IgD-Pacific Blue (11-26c.2a), IgD-BV605 (11-26c.2a), IgM-BV786
414 (II/41; BD), IgM-FITC (II/41), IgG1-BV650 (RMG1-1), IgG2b-PECy7 (RMG2b-1), IgG2c-
415 FITC (polyclonal; SouthernBiotech, Birmingham, AL), IL-4Rα-PE (REA235; Miltenyi Biotec),

416 and CD23-BV421 (B3B4). The following anti-human antibodies were used: IL-4Rα-PE
417 (G077F6), CD23-BV421 (EBVCS-5), IgD-AF700 (IA6-2), CD27-BV605 (O323), IgM-BV650
418 (MHM-88), CD38-PECy7 (HB-7), CD19-PerCP.Cy-5.5 (SJ25C1), CD3-BV711 (OKT3), CD14-
419 BV711 (M5E2), and CD16-BV711 (3G8). All antibodies were purchased from BioLegend (San
420 Diego, CA), unless otherwise noted. Viability staining was executed with Fixable Viability Dye
421 eFluor780 (eBioscience, San Diego, CA) or Fixable Viability Stain 510 (BD Biosciences).

422 Data were acquired with an LSRFortessa flow cytometer (BD). Bulk cell sorting was performed
423 on a MoFlo XDP cell sorter (Beckman Coulter, Brea, CA). All data were analyzed with FlowJo,
424 version 10 software (Tree Star, Ashland, OR).

425 **Adoptive Transfers**

426 Class-switched MBCs ($B220^+$ $CD3^-$ $F4/80^-$ $CD38^+$ $GL7^-$ IgD^- IgM^-) from tetramer enriched
427 fractions were isolated by flow sorting four weeks after donor immunization. 10^4 cells were
428 intravenously injected in the tail-vein of naïve recipient (muMT) mice. The day after transfer
429 recipients were intraperitoneally injected with 250 μg OVA with either 40 μg CpG or 5 μg CT.
430 One week later, spleens and mesenteric LNs were collected for flow cytometric analysis of donor
431 B cells, and serum was collected for OVA-specific antibody analysis by ELISA.

432 **ELISAs**

433 OVA-specific immunoglobulins were measured by sandwich ELISA, described previously, with
434 some modifications (*68*). Briefly, MaxiSorp plates (ThermoFisher Scientifc) were coated with
435 100 ng anti-IgG2b, -IgG2c, -IgE, or -IgA overnight at 4°C. Plates were blocked in 5% skim milk
436 at 37°C for one hour, then diluted samples were added and incubated overnight at 4°C.
437 Digoxigenated OVA (15 ng) prepared in-house was added for two hours at room temperature,

438 followed by anti-digoxigenin Fab fragments (Roche, Basel, Switzerland) for one hour. Plates
439 were developed with 3,3',5,5'-tetramethylbenzidinie (Sigma-Aldrich) and stopped with sulfuric
440 acid. Optical densities were acquired with a Multiskan FC photometer (ThermoFisher Scientific).

441 For OVA-IgG1, plates were coated with 400 ng OVA in carbonate-bicarbonate buffer overnight
442 at 4°C. Plates were blocked in 5% skim milk at 37°C for two hours, then diluted samples were
443 added and incubated overnight at 4°C. Biotinylated anti-mouse IgG1 (SouthernBiotech;1.25 ng)
444 was added for two hours at room temperature, followed by alkaline-phosphatase streptavidin
445 (ThermoFisher Scientific) for one hour. Plates were developed with 4-nitrophenyl phosphate
446 (Sigma-Aldrich) and stopped with sodium hydroxide. Optical densities were acquired as above.

447 **10x Chromium Sequencing & Analysis**

448 *Sequencing:* Spleens and inguinal LNs were collected one month post-recall response from
449 epicutaneously or subcutaneously sensitized mice and B cells were sorted for sequencing.
450 Single-cell 5' gene expression and V(D)J libraries were prepared with Chromium Single-Cell V3
451 Reagent Kit and Controller (10x Genomics; Pleasanton, CA). Libraries were sequenced with
452 NextSeq2000 (Illumina; San Diego, CA). Data were processed with the Cell Ranger Count and
453 V(D)J pipelines (version 7.0.1).

454 *Gene Expression Analysis:* Sequencing reads were aligned to the mouse transcriptome
455 (GRCm38), followed by filtering, and correction of cell barcodes and Unique Molecular
456 Identifiers (UMIs). Reads associated with retained barcodes were quantified and used to build
457 expression matrices for further analysis with Seurat (version 4.1.3). Cells expressing less than
458 200 genes, genes that were detected in less than 3 cells, and cells expressing over 10%
459 mitochondrial genes were filtered out. Normalization, variable feature selection, and scaling
460 were performed with Seurat default parameters. Principal component analysis (PCA) was

461 performed and the top 15 components were used for UMAP dimensionality reduction and
462 clustering at resolution 0.4. Contaminating non-B cells were filtered out and PCA and clustering
463 were repeated on the subsetted Seurat object at resolution 0.3. Differentially expressed genes or
464 gene modules were identified with the Wilcoxon Rank Sum test.

465 *BCR Analysis:* BCR analysis was performed with pipelines in the Immcantation suite (*46*). The
466 "filtered_contig.fasta" and "filtered_contig_annotations.csv" outputs from Cell Ranger V(D)J
467 were used to assign V, D, and J genes with IgBLAST and cells assigned with 0 or >1 heavy
468 chains were removed. Clonal groups were defined with the hierarchialClones function using
469 applying a Hamming distance of 0.1. Germline sequences were reconstructed with
470 createGermlines and IMGT germline references (version 3.1.39). Somatic hypermutation
471 frequency within the IGHV gene was calculated with observedMutations.

472 **Bulk VDJ Sequencing & Analysis**

473 *Sequencing:* Spleens and inguinal LNs were collected one month post-recall response from
474 epicutaneously sensitized mice. ~12,000-15,000 B cells from the tetramer-enriched fraction were
475 sorted directly into Buffer RLT (Qiagen; Hilden, DE) prior to shipment on dry ice to iRepertoire.
476 RNA extraction was performed prior to 3-chain long read library preparation (Mouse BCR
477 Heavy, Kappa, Lambda). Amplified PCR products were run on MiSeq System with MiSeq
478 Reagent Nano Kit v2 (iRepertoire, Huntsville, AL).

479 *Analysis:* Nucleotide sequences and UMI count were extracted from "joinedSeq" and "copy"
480 columns of the "pep.csv" output from iRweb (iRepertoire) and were aligned with IgBLAST
481 (version 1.18.0) using IMGT reference sequences. Processing of IgBLAST output was
482 performed with the Immcantation suite to assign V, D, and J genes, cluster into clonal groups,
483 assign unmutated germlines, and calculate IGHV somatic hypermutation frequency, as described

484 in the 10x Chromium section. Lineage tree topologies were predicted by maximum parsimony in
485 IgPhyML with constraints for unidirectional isotype switching and trees were subsequently
486 visualized with dowser (*69*, *70*).

487 **Smart-Seq2 Sequencing & Analysis**

488 *Sequencing:* Spleens and inguinal LNs were collected one month post-recall response from
489 epicutaneously sensitized mice. OVA-specific B cells were-single cell sorted into 96 U-bottom
490 well PCR-grade RNase and DNase free plates before being flash frozen at -80C. Full-length
491 cDNA was generated with Smart-Seq Single Cell Kit (Takarabio; Mountain View, CA).
492 Libraries were then prepared for sequencing with NovaSeq 600 Reagent Kits (Illumina;
493 20028400) and sequenced on Illumina NovaSeq 6000 (Ilumina; San Diego, CA).

494 *Analysis:* Sequencing reads were aligned to the mouse transcriptome (GRCm38) with STARsolo
495 (*71*). Count matrix output was normalized and scaled with Seurat (version 4.1.3). BCR
496 sequences were reconstructed with the TRUST4 algorithm, followed by integration with the gene
497 expression data using Platypus (*72*, *73*)

498 **Statistical Analysis**

499 Statistical analyses not pertaining to RNA sequencing were performed with Prism 9 (GraphPad
500 Software; San Diego, CA). Comparisons were drawn between groups (CT, IC, A4RA) or across
501 time points using two-sided Student's *t*-test or ANOVA. Data were considered significant with a
502 p value < 0.05.

List of Supplementary Materials

Fig. S1. Gene expression profiles of naïve B cell clusters.

Fig. S2. Requirement of B-T interactions for IgE recall responses.

Fig. S3. Analysis of publicly reposited scRNA-seq datasets.

Fig. S4. B cell reprogramming in orally-sensitized mice.

Fig. S5. VDJ repertoire analysis in OVA-enriched bulk sequencing and 10X datasets.

References and Notes

1. R. R. Goel, S. A. Apostolidis, M. M. Painter, D. Mathew, A. Pattekar, O. Kuthuru, S. Gouma, P. Hicks, W. Meng, A. M. Rosenfeld, S. Dysinger, K. A. Lundgreen, L. Kuri-Cervantes, S. Adamski, A. Hicks, S. Korte, D. A. Oldridge, A. E. Baxter, J. R. Giles, M. E. Weirick, C. M. McAllister, J. Dougherty, S. Long, K. D'Andrea, J. T. Hamilton, M. R. Betts, E. T. Luning Prak, P. Bates, S. E. Hensley, A. R. Greenplate, E. J. Wherry, Distinct antibody and memory B cell responses in SARSCoV-2 naïve and recovered individuals following mRNA vaccination. *Sci Immunol* **6**, 1–19 (2021).
2. J. Wrammert, K. Smith, J. Miller, W. A. Langley, K. Kokko, C. Larsen, N. Y. Zheng, I. Mays, L. Garman, C. Helms, J. James, G. M. Air, J. D. Capra, R. Ahmed, P. C. Wilson, Rapid cloning of high-affinity human monoclonal antibodies against influenza virus. *Nature 2008 453:7195* **453**, 667–671 (2008).
3. T. Onodera, Y. Takahashi, Y. Yokoi, M. Ato, Y. Kodama, S. Hachimura, T. Kurosaki, K. Kobayashi, Memory B cells in the lung participate in protective humoral immune responses to pulmonary influenza virus reinfection. *Proc Natl Acad Sci U S A* **109**, 2485–2490 (2012).
4. Z. Yang, B. M. Sullivan, C. D. C. Allen, Fluorescent in vivo detection reveals that IgE(+) B cells are restrained by an intrinsic cell fate predisposition. *Immunity* **36**, 857–72 (2012).
5. R. Jiménez-Saiz, D. K. Chu, T. S. Mandur, T. D. Walker, M. E. Gordon, R. Chaudhary, J. Koenig, S. Saliba, H. J. Galipeau, A. Utley, I. L. King, K. Lee, R. Ettinger, S. Waserman, R. Kolbeck, M. Jordana, Lifelong Memory Responses Perpetuate Humoral Th2 Immunity and Anaphylaxis in Food Allergy. *Journal of Allergy and Clinical Immunology* **140**, 1604–1615 (2017).
6. N. Carballeda-Sangiao, A. I. Rodríguez-Mahillo, M. Careche, A. Navas, I. Moneo, M. González-Muñoz, Changes over Time in IgE Sensitization to Allergens of the Fish Parasite Anisakis spp. *PLoS Negl Trop Dis* **10**, e0004864 (2016).
7. M. S. Kim, M. D. Straesser, B. Keshavarz, L. Workman, E. C. McGowan, T. A. E. Platts-Mills, J. M. Wilson, IgE to galactose-α-1,3-galactose wanes over time in patients who avoid tick bites. *J Allergy Clin Immunol Pract* **8**, 364-367.e2 (2020).
8. D. L. Neuman-Sunshine, J. A. Eckman, C. A. Keet, E. C. Matsui, R. D. Peng, P. J. Lenehan, R. A. Wood, The natural history of persistent peanut allergy. *Annals of Allergy, Asthma & Immunology* **108**, 326-331.e3 (2012).
9. T. J. Looney, J.-Y. Lee, K. M. Roskin, R. A. Hoh, J. King, J. Glanville, Y. Liu, T. D. Pham, C. L. Dekker, M. M. Davis, S. D. Boyd, Human B-cell isotype switching origins of IgE. *J Allergy Clin Immunol* **137**, 579-586.e7 (2016).
10. J.-S. He, S. Subramaniam, V. Narang, K. Srinivasan, S. P. Saunders, D. Carbajo, T. Wen-Shan, N. Hidayah Hamadee, J. Lum, A. Lee, J. Chen, M. Poidinger, F. Zolezzi, J. J. Lafaille, M. A. Curotto de Lafaille, IgG1 memory B cells keep the memory of IgE responses. *Nat Commun* **8**, 641 (2017).
11. I. Hoof, V. Schulten, J. A. Layhadi, T. Stranzl, L. H. Christensen, S. Herrera de la Mata, G. Seumois, P. Vijayanand, C. Lundegaard, K. Niss, A. Lund, J. Ahrenfeldt, J. Holm, E. Steveling, H. Sharif, S. R. Durham,

538 B. Peters, M. H. Shamji, P. S. Andersen, Allergen-specific IgG+ memory B cells are temporally linked to
539 IgE memory responses. *J Allergy Clin Immunol* **146**, 180–191 (2020).
540 12. C. J. Aranda, E. Gonzalez-Kozlova, S. P. Saunders, W. Fernandes-Braga, M. Ota, S. Narayanan, J. S. He, E.
541 Del Duca, B. Swaroop, S. Gnjatic, G. Shattner, J. Reibman, N. A. Soter, E. Guttman-Yassky, M. A. Curotto
542 de Lafaille, IgG memory B cells expressing IL4R and FCER2 are associated with atopic diseases. *Allergy*
543 **00**, 1–15 (2022).
544 13. J. F. E. Koenig, N. P. H. Knudsen, A. Phelps, K. Bruton, I. Hoof, G. Lund, D. Della Libera, A. Lund, L. H.
545 Christensen, D. R. Glass, T. Walker, A. Fang, S. Waserman, M. Jordana, P. S. Andersen, A Distinct
546 Phenotype of Polarized Memory B cell holds IgE Memory. *bioRxiv*, 2023.01.25.525495 (2023).
547 14. M. Ota, K. B. Hoehn, T. Ota, C. J. Aranda, S. Friedman, W. F. Braga, A. Malbari, S. H. Kleinstein, S. H.
548 Sicherer, M. A. C. de Lafaille, The memory of pathogenic IgE is contained within CD23+IgG1+ memory B
549 cells poised to switch to IgE in food allergy. *bioRxiv*, 2023.01.25.525506 (2023).
550 15. F. D. Finkelman, J. F. Urban, M. P. Beckmann, K. A. Schooley, J. M. Holmes, I. M. Katona, Regulation of
551 murine in vivo IgG and IgE responses by a monoclonal anti-IL-4 receptor antibody. *Int Immunol* **3**, 599–607
552 (1991).
553 16. F. D. Finkelman, I. M. Katona, J. F. Urban, J. Holmes, J. Ohara, A. S. Tung, J. Sample vG., W. E. Paul, IL-4
554 is required to generate and sustain in vivo IgE responses. *J Immunol* (1988).
555 17. K. Bruton, P. Spill, S. Vohra, O. Baribeau, S. Manzoor, S. Gadkar, M. Davidson, T. D. Walker, J. F. E.
556 Koenig, Y. Ellenbogen, A. Florescu, J. Wen, D. K. Chu, S. Waserman, R. Jiménez-Saiz, S. Epelman, C.
557 Robbins, M. Jordana, Interrupting reactivation of immunologic memory diverts the allergic response and
558 prevents anaphylaxis. *J Allergy Clin Immunol* **147**, 1381–1392 (2021).
559 18. J. K. Nono, H. Ndlovu, N. Abdel Aziz, T. Mpotje, L. Hlaka, F. Brombacher, Interleukin-4 receptor alpha is
560 still required after Th2 polarization for the maintenance and the recall of protective immunity to Nematode
561 infection. *PLoS Negl Trop Dis* **11** (2017).
562 19. I. M. Katona, J. F. Urban, S. S. Kang, W. E. Paul, F. D. Finkelman, IL-4 requirements for the generation of
563 secondary in vivo IgE responses. *J Immunol* **146**, 4215–21 (1991).
564 20. R. Jiménez-Saiz, Y. Ellenbogen, J. Koenig, M. E. Gordon, T. D. Walker, D. Rosace, P. Spill, K. Bruton, J.
565 Kong, K. Monteiro, J. Wen, E. I. Tuomanen, R. Kolbeck, D. K. Chu, S. Waserman, M. Jordana, IgG1 $^{+}$ B
566 cell immunity predates IgE responses in epicutaneous sensitization to foods. *Allergy*, doi: 10.1111/all.13481
567 (2018).
568 21. K. Haniuda, S. Fukao, D. Kitamura, Metabolic Reprogramming Induces Germinal Center B Cell
569 Differentiation through Bcl6 Locus Remodeling. *Cell Rep* **33** (2020).
570 22. L. R. Waters, F. M. Ahsan, D. M. Wolf, O. Shirihai, M. A. Teitell, Initial B Cell Activation Induces
571 Metabolic Reprogramming and Mitochondrial Remodeling. *iScience* **5**, 99 (2018).
572 23. R. Noelle, P. H. Krammer, J. Ohara, J. W. Uhr, E. S. Vitetta, Increased expression of Ia antigens on resting
573 B cells: an additional role for B-cell growth factor. *Proceedings of the National Academy of Sciences* **81**,
574 6149–6153 (1984).
575 24. S. R. Dillon, C. Sprecher, A. Hammond, J. Bilsborough, M. Rosenfeld-Franklin, S. R. Presnell, H. S.
576 Haugen, M. Maurer, B. Harder, J. Johnston, S. Bort, S. Mudri, J. L. Kuijper, T. Bukowski, P. Shea, D. L.
577 Dong, M. Dasovich, F. J. Grant, L. Lockwood, S. D. Levin, C. LeCiel, K. Waggie, H. Day, S. Topouzis, J.
578 Kramer, R. Kuestner, Z. Chen, D. Foster, J. Parrish-Novak, J. A. Gross, Interleukin 31, a cytokine produced
579 by activated T cells, induces dermatitis in mice. *Nature Immunology 2004 5:7* **5**, 752–760 (2004).
580 25. D. Chen, Y. Wang, G. K. Manakkat Vijay, S. Fu, C. W. Nash, D. Xu, D. He, N. Salomonis, H. Singh, H.
581 Xu, Coupled analysis of transcriptome and BCR mutations reveals role of OXPHOS in affinity maturation.
582 *Nature Immunology 2021 22:7* **22**, 904–913 (2021).
583 26. S. C. Choi, L. Morel, Immune metabolism regulation of the germinal center response. *Experimental &*
584 *Molecular Medicine 2020 52:3* **52**, 348–355 (2020).
585 27. A. Turqueti-Neves, M. Otte, O. P. da Costa, U. E. Höpken, M. Lipp, T. Buch, D. Voehringer, B-cell-
586 intrinsic STAT6 signaling controls germinal center formation. *Eur J Immunol* **44**, 2130–2138 (2014).
587 28. C. AF, S. K, T. KM, K. M, A. J, B. F, M. ICM, Pinpointing IL-4-independent acquisition and IL-4-
588 influenced maintenance of Th2 activity by CD4 T cells. *Eur J Immunol* **34** (2004).
589 29. G. v Zuccarino-Catania, S. Sadanand, F. J. Weisel, M. M. Tomayko, H. Meng, S. H. Kleinstein, K. L. Good-
590 Jacobson, M. J. Shlomchik, CD80 and PD-L2 define functionally distinct memory B cell subsets that are
591 independent of antibody isotype. *Nat Immunol* **15**, 631–637 (2014).

30. J. J. Taylor, R. J. Martinez, P. J. Titcombe, L. O. Barsness, S. R. Thomas, N. Zhang, S. D. Katzman, M. K. Jenkins, D. L. Mueller, Deletion and anergy of polyclonal B cells specific for ubiquitous membrane-bound self-antigen. *J Exp Med* **209**, 2065–77 (2012).
31. J. J. Taylor, K. A. Pape, M. K. Jenkins, A germinal center-independent pathway generates unswitched memory B cells early in the primary response. *J Exp Med* **209**, 597–606 (2012).
32. L. Duan, D. Liu, H. Chen, M. A. Mintz, M. Y. Chou, D. I. Kotov, Y. Xu, J. An, B. J. Laidlaw, J. G. Cyster, Follicular dendritic cells restrict interleukin-4 availability in germinal centers and foster memory B cell generation. *Immunity* **54**, 2256-2272.e6 (2021).
33. J. D. Mountz, M. Gao, D. M. Ponder, S. Liu, C. W. Sun, F. Alduraibi, K. Sullivan, B. Pat, L. J. Dell'Italia, H. C. Hsu, IL-4 receptor blockade is a global repressor of naïve B cell development and responses in a dupilumab-treated patient. *Clin Immunol* **244** (2022).
34. M. Sarfati, S. Fournier, M. Christoffersen, G. Biron, Expression of CD23 antigen and its regulation by IL-4 in chronic lymphocytic leukemia. *Leuk Res* **14**, 47–55 (1990).
35. J.-S. He, M. Meyer-Hermann, D. Xiangying, L. Y. Zuan, L. A. Jones, L. Ramakrishna, V. C. de Vries, J. Dolpady, H. Aina, S. Joseph, S. Narayanan, S. Subramaniam, M. Puthia, G. Wong, H. Xiong, M. Poidinger, J. F. Urban, J. J. Lafaille, M. A. Curotto de Lafaille, The distinctive germinal center phase of IgE+ B lymphocytes limits their contribution to the classical memory response. *Journal of Experimental Medicine* **210**, 2755–2771 (2013).
36. Z. Yang, M. J. Robinson, C. D. C. Allen, Regulatory constraints in the generation and differentiation of IgE-expressing B cells. *Curr Opin Immunol* **28**, 64–70 (2014).
37. A. K. Gloudemans, M. Plantinga, M. Guilliams, M. A. Willart, A. Ozir-Fazalalikhan, A. van der Ham, L. Boon, N. L. Harris, H. Hammad, H. C. Hoogsteden, M. Yazdanbakhsh, R. W. Hendriks, B. N. Lambrecht, H. H. Smits, The Mucosal Adjuvant Cholera Toxin B Instructs Non-Mucosal Dendritic Cells to Promote IgA Production Via Retinoic Acid and TGF-β. *PLoS One* **8**, e59822 (2013).
38. T. M. McIntyre, D. R. Klinma, P. Rohman, M. Lugo, J. R. Dasch, J. J. Mond, C. M. Snapper, Transforming growth factor beta 1 selectivity stimulates immunoglobulin G2b secretion by lipopolysaccharide-activated murine B cells. *Journal of Experimental Medicine* **177**, 1031–1037 (1993).
39. C. M. Snapper, W. E. Paul, Interferon-γ and B Cell Stimulatory Factor-1 Reciprocally Regulate Ig Isotype Production. *Science (1979)* **236**, 944–947 (1987).
40. A. Bossie, E. S. Vitetta, IFN-gamma enhances secretion of IgG2a from IgG2a-committed LPS-stimulated murine B cells: implications for the role of IFN-gamma in class switching. *Cell Immunol* **135**, 95–104 (1991).
41. D. Esterházy, M. C. C. Canesso, L. Mesin, P. A. Muller, T. B. R. de Castro, A. Lockhart, M. ElJalby, A. M. C. Faria, D. Mucida, Compartmentalized gut lymph node drainage dictates adaptive immune responses. *Nature 2019 569:7754* **569**, 126–130 (2019).
42. B. Zhang, E. Liu, J. A. Gertie, J. Joseph, L. Xu, E. Y. Pinker, D. A. Waizman, J. Catanzaro, K. H. Hamza, K. Lahl, U. Gowthaman, S. C. Eisenbarth, Divergent T follicular helper cell requirement for IgA and IgE production to peanut during allergic sensitization. *Sci Immunol* **5** (2020).
43. Q. Chen, M. Xie, H. Liu, A. L. Dent, Development of allergen-specific IgE in a food-allergy model requires precisely timed B cell stimulation and is inhibited by Fgl2. *Cell Rep* **39**, 110990 (2022).
44. M. Vajdy, M. H. Kosco-Vilbois, M. Kopf, G. Köhler, N. Lycke, Impaired mucosal immune responses in interleukin 4-targeted mice. *J Exp Med* **181**, 41–53 (1995).
45. Z. Chen, A. M. Collins, Y. Wang, B. A. Gata, Clustering-based identification of clonally-related immunoglobulin gene sequence sets. *Immunome Res* **6**, 1–7 (2010).
46. N. T. Gupta, J. A. Vander Heiden, M. Uduman, D. Gadala-Maria, G. Yaari, S. H. Kleinstein, Change-O: a toolkit for analyzing large-scale B cell immunoglobulin repertoire sequencing data. *Bioinformatics* **31**, 3356–3358 (2015).
47. Z. Yang, C.-A. M. Wu, S. Targ, C. D. C. Allen, IL-21 is a broad negative regulator of IgE class switch recombination in mouse and human B cells. *Journal of Experimental Medicine* **217** (2020).
48. R. Jiménez-Saiz, Y. Ellenbogen, K. Bruton, P. Spill, D. D. Sommer, H. Lima, S. Waserman, S. U. Patil, W. G. Shreffler, M. Jordana, Human BCR analysis of single-sorted, putative IgE+ memory B cells in food allergy. *J Allergy Clin Immunol* **144**, 336-339.e6 (2019).
49. L. Shehata, C. D. Thouvenel, B. D. Hondowicz, L. A. Pew, D. J. Rawlings, J. Choi, M. Pepper, IL-4 downregulates BCL6 to promote memory B cell selection in germinal centers. *bioRxiv*, 2023.01.26.525749 (2023).

50. D. G. Gonzalez, C. M. Cote, J. R. Patel, C. B. Smith, Y. Zhang, K. M. Nickerson, T. Zhang, S. M. Kerfoot, A. M. Haberman, Nonredundant Roles of IL-21 and IL-4 in the Phased Initiation of Germinal Center B Cells and Subsequent Self-Renewal Transitions. *J Immunol* **201**, 3569–3579 (2018).
51. B. G. De Jong, H. Ijspeert, L. Marques, M. Van Der Burg, J. J. M. Van Dongen, B. G. Loos, M. C. Van Zelm, Human IgG2- and IgG4-expressing memory B cells display enhanced molecular and phenotypic signs of maturity and accumulate with age. *Immunol Cell Biol* **95**, 744 (2017).
52. A. M. Collins, K. J. L. Jackson, A Temporal Model of Human IgE and IgG Antibody Function. *Front Immunol* **4** (2013).
53. D. MacGlashan, R. G. Hamilton, Parameters Determining the Efficacy of CD32 to Inhibit Activation of FcεRI in Human Basophils. *J Allergy Clin Immunol* **137**, 1256 (2016).
54. M. Sugimoto, N. Kamemura, M. Nagao, M. Irahara, S. Kagami, T. Fujisawa, H. Kido, Differential response in allergen-specific IgE, IgGs, and IgA levels for predicting outcome of oral immunotherapy. *Pediatr Allergy Immunol* **27**, 276–282 (2016).
55. J. J. Heeringa, C. I. McKenzie, N. Varese, M. Hew, A. T. C. M. Bakx, P. M. Aui, J. M. Rolland, R. E. O'Hehir, M. C. van Zelm, Induction of IgG2 and IgG4 B-cell memory following sublingual immunotherapy for ryegrass pollen allergy. *Allergy* **75**, 1121 (2020).
56. O. T. Burton, S. L. Logsdon, J. S. Zhou, J. Medina-Tamayo, A. Abdel-Gadir, M. Noval Rivas, K. J. Koleoglou, T. A. Chatila, L. C. Schneider, R. Rachid, D. T. Umetsu, H. C. Oettgen, Oral immunotherapy induces IgG antibodies that act via FcγRIIb to suppress IgE-mediated hypersensitivity. *J Allergy Clin Immunol* **134**, 1310 (2014).
57. E. Wambre, V. Bajzik, J. H. DeLong, K. O'Brien, Q.-A. Nguyen, C. Speake, V. H. Gersuk, H. A. DeBerg, E. Whalen, C. Ni, M. Farrington, D. Jeong, D. Robinson, P. S. Linsley, B. P. Vickery, W. W. Kwok, A phenotypically and functionally distinct human TH2 cell subpopulation is associated with allergic disorders. *Sci Transl Med* **9**, eaam9171 (2017).
58. C. Bangert, K. Rindler, T. Krausgruber, N. Alkon, F. M. Thaler, H. Kurz, T. Ayub, D. Demirtas, N. Fortelny, V. Vorstandlechner, W. M. Bauer, T. Quint, M. Mildner, C. Jonak, A. Elbe-Bürger, J. Griss, C. Bock, P. M. Brunner, Persistence of mature dendritic cells, T_H2A, and Tc2 cells characterize clinically resolved atopic dermatitis under IL-4Rα blockade. *Sci Immunol* **6** (2021).
59. H. Renz, J. Domenico, E. W. Gelfand, IL-4-dependent up-regulation of IL-4 receptor expression in murine T and B cells. *Journal of Immunology* **146**, 3049–3055 (1991).
60. J. Holm, N. Willumsen, P. A. Würtzen, L. H. Christensen, K. Lund, Facilitated antigen presentation and its inhibition by blocking IgG antibodies depends on IgE repertoire complexity. *J Allergy Clin Immunol* **127**, 1029–37 (2011).
61. C. Liu, K. Richard, M. Wiggins, X. Zhu, D. H. Conrad, W. Song, CD23 can negatively regulate B-cell receptor signaling. *Sci Rep* **6**, 25629 (2016).
62. F. Horns, C. Vollmers, D. Croote, S. F. Mackey, G. E. Swan, C. L. Dekker, M. M. Davis, S. R. Quake, Lineage tracing of human B cells reveals the in vivo landscape of human antibody class switching. *Elife* **5** (2016).
63. P. Irrgang, J. Gerling, K. Kocher, D. Lapuente, P. Steininger, K. Habenicht, M. Wytopil, S. Beileke, S. Schäfer, J. Zhong, G. Ssebyatika, T. Krey, V. Falcone, C. Schülein, A. S. Peter, K. Nganou-Makamdop, H. Hengel, J. Held, C. Bogdan, K. Überla, K. Schober, T. H. Winkler, M. Tenbusch, Class switch toward noninflammatory, spike-specific IgG4 antibodies after repeated SARS-CoV-2 mRNA vaccination. *Sci Immunol* **8** (2023).
64. B. P. Vickery, J. Lin, M. Kulis, Z. Fu, P. H. Steele, S. M. Jones, A. M. Scurlock, G. Gimenez, L. Bardina, H. A. Sampson, A. W. Burks, Peanut oral immunotherapy modifies IgE and IgG4 responses to major peanut allergens. *J Allergy Clin Immunol* **131**, 128-34.e1–3 (2013).
65. P. Varshney, S. M. Jones, A. M. Scurlock, T. T. Perry, A. Kemper, P. Steele, A. Hiegel, J. Kamilaris, S. Carlisle, X. Yue, M. Kulis, L. Pons, B. Vickery, A. W. Burks, A randomized controlled study of peanut oral immunotherapy: clinical desensitization and modulation of the allergic response. *J Allergy Clin Immunol* **127**, 654–60 (2011).
66. T. Rispens, M. G. Huijbers, The unique properties of IgG4 and its roles in health and disease. *Nature Reviews Immunology 2023 23:11* **23**, 763–778 (2023).
67. K. Arias, D. K. Chu, K. Flader, F. Botelho, T. D. Walker, N. Arias, A. A. Humbles, A. J. Coyle, H. C. Oettgen, H.-D. Chang, N. van Rooijen, S. Waserman, M. Jordana, Distinct immune effector pathways contribute to the full expression of peanut-induced anaphylactic reactions in mice. *J Allergy Clin Immunol* **127**, 1552–61.e1 (2011).

68. J. Sun, K. Arias, D. Alvarez, R. Fattouh, T. Walker, S. Goncharova, B. Kim, S. Waserman, J. Reed, A. J. Coyle, M. Jordana, Impact of CD40 Ligand, B Cells, and Mast Cells in Peanut-Induced Anaphylactic Responses. *The Journal of Immunology* **179** (2007).
69. K. B. Hoehn, J. A. Vander Heiden, J. Q. Zhou, G. Lunter, O. G. Pybus, S. H. Kleinstein, Repertoire-wide phylogenetic models of B cell molecular evolution reveal evolutionary signatures of aging and vaccination. *Proc Natl Acad Sci U S A* **116**, 22664–22672 (2019).
70. K. B. Hoehn, O. G. Pybus, S. H. Kleinstein, Phylogenetic analysis of migration, differentiation, and class switching in B cells. *PLoS Comput Biol* **18** (2022).
71. B. Kaminow, D. Yunusov, A. Dobin, STARsolo: accurate, fast and versatile mapping/quantification of single-cell and single-nucleus RNA-seq data. *bioRxiv*, 2021.05.05.442755 (2021).
72. L. Song, D. Cohen, Z. Ouyang, Y. Cao, X. Hu, X. S. Liu, TRUST4: immune repertoire reconstruction from bulk and single-cell RNA-seq data. *Nature Methods 2021 18:6* **18**, 627–630 (2021).
73. A. Yermanos, A. Agrafiotis, R. Kuhn, D. Robbiani, J. Yates, C. Papadopoulou, J. Han, I. Sandu, C. Weber, F. Bieberich, R. Vazquez-Lombardi, A. Dounas, D. Neumeier, A. Oxenius, S. T. Reddy, Platypus: an open-access software for integrating lymphocyte single-cell immune repertoires with transcriptomes. *NAR Genom Bioinform* **3** (2021).

Acknowledgments: We kindly thank S. Eisenbarth for thoughtful review of the manuscript. We also thank M. Subapanditha and for assistance with cell sorting and C. Mader, the McMaster Genomics Facility, and G. Kongsgaard Koed, and J. Skovsgaard for sequencing support. Experimental schematics were created with BioRender (www.biorender.com). KB was supported by a CIHR CGS-Doctoral award and CIHR Postdoctoral Fellowship. AP was supported by the Schroder Allergy & Immunology Research Institute Scholarship and an Ontario Graduate Scholarship.

Funding:

Schroeder Foundation (SW, MJ)

Food Allergy Canada (SW, MJ)

ALK Abelló (SW, MJ)

Canadian Allergy, Asthma, and Immunology Foundation (MJ)

Michael Zych Family (SW, MJ)

Author contributions:

Conceptualization: KB, AP, MJ

Investigation: KB, AP, AA, TDW, JW, SSK-B, AF, OM-D, SG, EG, JFEK, AG

Visualization: KB, AP

Funding acquisition: SW, PSA, MJ

Supervision: MJ

Writing – original draft: KB, AP

Writing – review & editing: KB, AP

Competing interests: JFEK, SW, and MJ receive funding from ALK Abelló A/S. All other authors declare that they have no competing interests.

Data and materials availability: This manuscript produced no new code. Single-cell and bulk sequencing data will be deposited to the GEO database prior to publication. All other data are available within the main text or the supplementary materials.

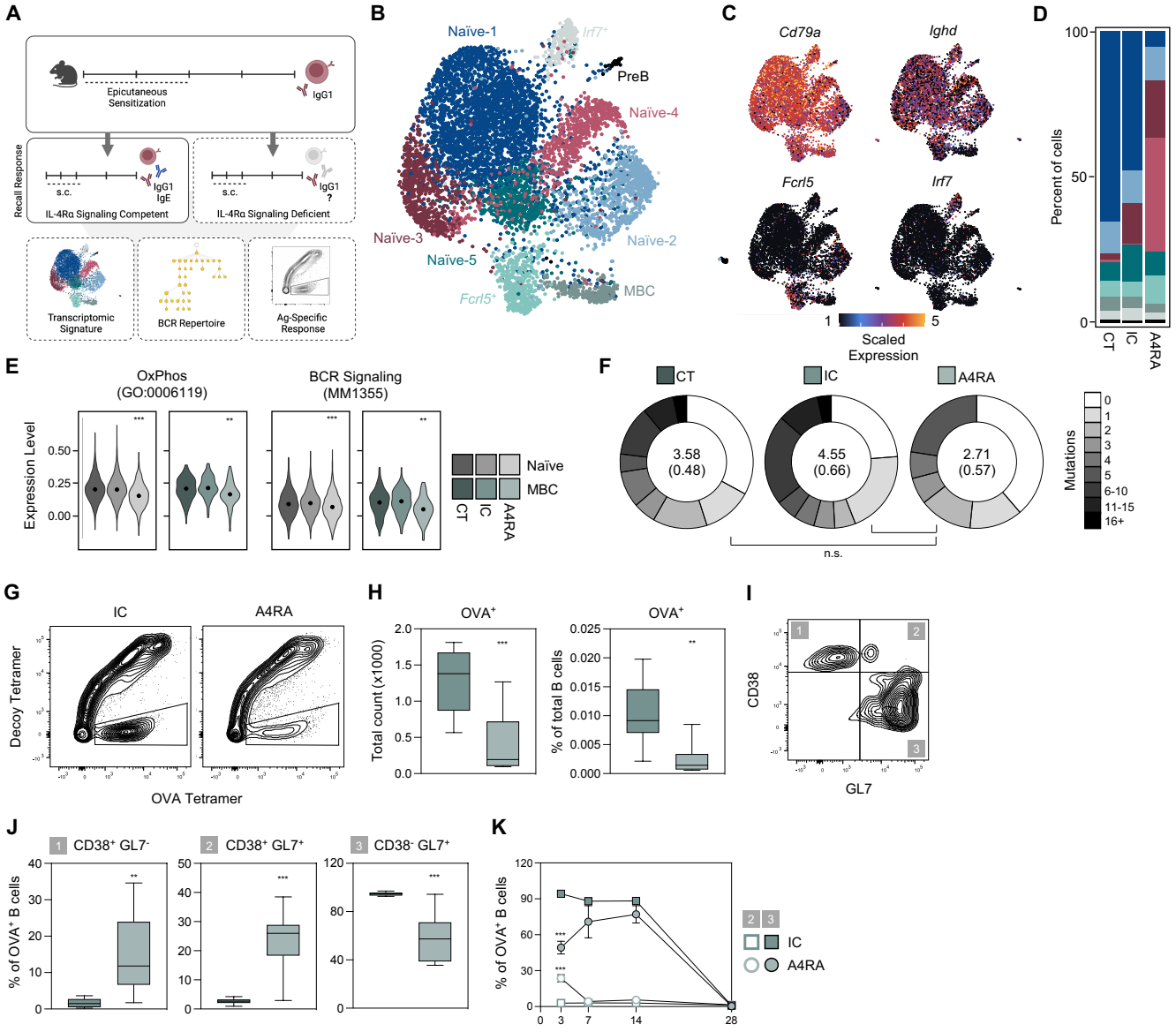
A
Epicutaneous Sensitization
IgG1
Recall Response
s.c.
IgG1
IgE
IL-4Rα Signaling Competent
s.c.
IgG1
?
IL-4Rα Signaling Deficient
Transcriptomic Signature
BCR Repertoire
Ag-Specific Response
B
Naïve-1
Irf7+
PreB
Naïve-4
Naïve-3
Naïve-5
Naïve-2
Fcrl5+
MBC
C
Cd79a
Ighd
Fcrl5
Irf7
1
5
Scaled Expression
D
Percent of cells
100
50
0
CT
IC
A4RA
E
OxPhos (GO:0006119)
BCR Signaling (MM1355)
Expression Level
0.50
0.25
0.00
Naïve
MBC
CT
IC
A4RA
F
CT
IC
A4RA
3.58 (0.48)
4.55 (0.66)
2.71 (0.57)
n.s.
Mutations
0
1
2
3
4
5
6-10
11-15
16+
G
IC
A4RA
Decoy Tetramer
OVA Tetramer
H
OVA+
Total count (x1000)
OVA+
% of total B cells
I
CD38
GL7
J
1 CD38+ GL7-
2 CD38+ GL7+
3 CD38- GL7+
% of OVA+ B cells
K
% of OVA+ B cells
0
3
7
14
28
IC
A4RA

719 **Fig. 1**. **IL-4Rα signaling augments secondary germinal center activity. (A)** Study schematic.
720 **(B)** UMAP of B cell clusters from scRNA-seq analysis of B cells isolated from spleens and
721 inguinal LNs of CT-immunized mice and A4RA/IC-treated epicutaneously sensitized mice. $n = 5$
722 CT, $n = 10$ IC, $n = 10$ A4RA. **(C)** UMAP plots of genes defining naïve and MBC clusters. **(D)**
723 Percent of cells in each cluster by treatment group. **(E)** Expression level of gene modules in
724 naïve B cell clusters 1-5 (grey) and MBCs (green) by treatment group. Point indicates median.
725 **(F)** VDJ analysis of MBCs identifying the number of nucleotide mutations compared to the
726 germline sequence. Shading in circle plots depict the fraction of cells with each number of
727 mutations. Mean (SEM) number of mutations are displayed within the circles. **(G)**
728 Representative contour plots of enriched OVA^+ B cell population from inguinal LNs of
729 epicutaneously sensitized mice. Pre-gated as live > singlet > $F4/80^-$ $CD3^-$ > $B220^+$. **(H)** Summary
730 plots of OVA^+ B cell total count and frequency. **(I)** Representative contour plot of resting
731 ($CD38^+$ $GL7^-$), transitional ($CD38^+$ $GL7^+$) and germinal center ($CD38^-$ $GL7^+$) B cells. Pre-gated
732 from OVA^+ B cells > IgM^- IgD^-. **(J)** Summary plots of OVA^+ B cell frequency within the
733 populations from (I) at three days post-boost. **(K)** Summary plot of OVA^+ B cell frequency
734 within transitional (empty) and germinal center (filled) populations in post-boost time course.
735 Data represent 2 experiments, each with 4 mice per group. Data are presented as median ±
736 min/max (H, J) or mean ± SEM (K). ** $p < 0.01$, *** $p < 0.001$.

A

	Duan & Liu *et al.* 2021		Bruton & Spill *et al.* 2021	Mountz & Gao *et al.* 2022
	LSC Il4r Deficiency	***In vivo* A4RA**	***In vitro* A4RA**	**Dupilumab Trial**
Species	Mouse	Mouse	Human	Human
Allergy	NP_{14}-CGG	OVA	Peanut	Atopic Dermatitis
Intervention	Ccl19-*Il4ra*$^{-/-}$	Ab Blockade	Ab Blockade	Ab Blockade
IL-4 Signaling	↑	X	X	X
Ag Re-Exposure	+	+	+	-

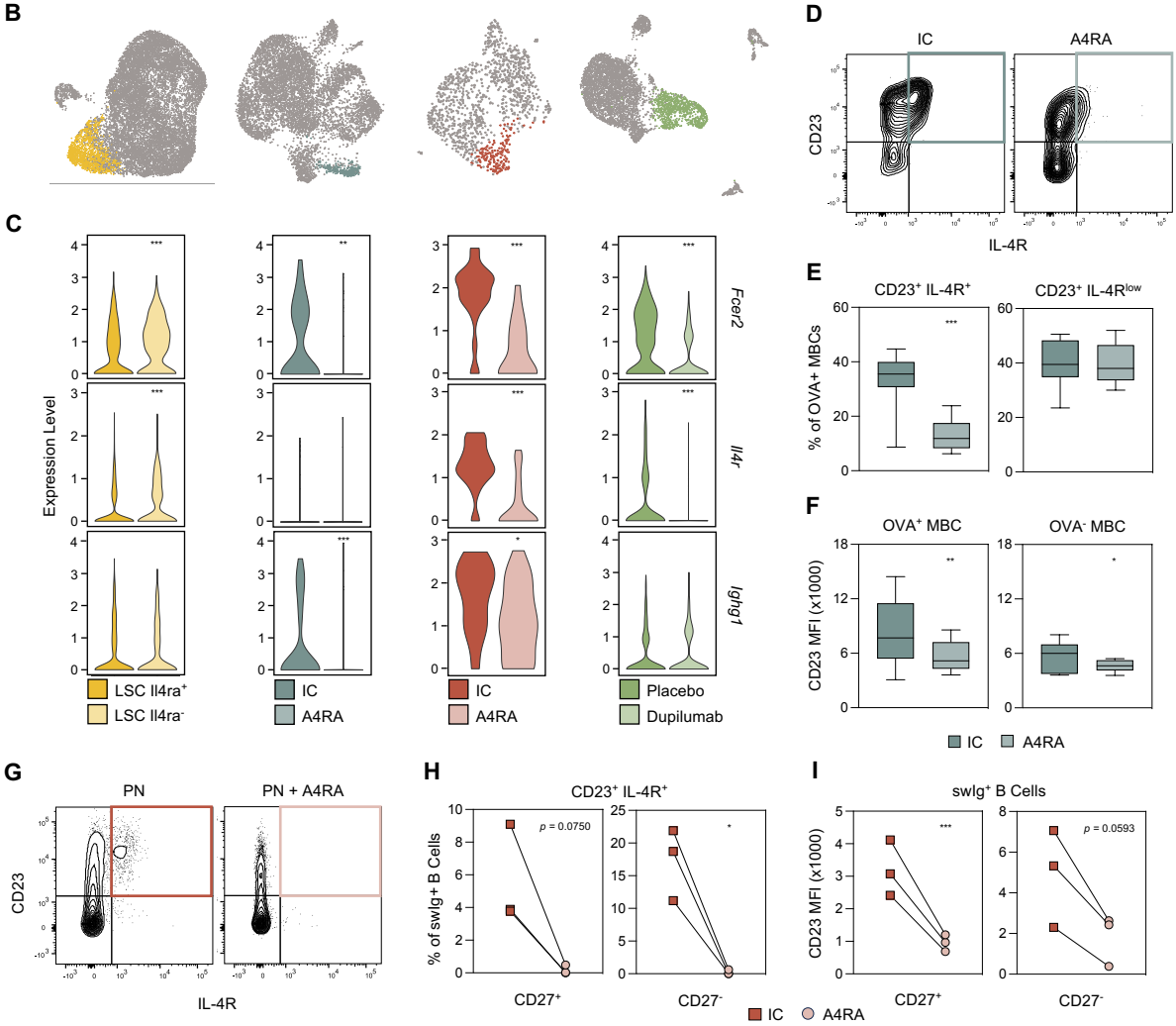

737 **Fig. 2. MBC2 phenotype is ameliorated with IL-4Rα blockade in mice and humans. (A)**
738 Overview of analyzed datasets. **(B)** UMAP of B cell clusters from scRNA-seq data sets. Colored
739 points indicate class-switched cluster used for downstream analyses. **(C)** Expression level of
740 MBC2-related genes in MBC clusters. **(D)** Representative contour plots of OVA^+ MBC2s from
741 inguinal LNs of epicutaneously sensitized mice four weeks after re-exposure and antibody
742 treatment. Pre-gated as OVA^+ B cells > $CD38^+$ $GL7^-$ > IgM^- IgD^-. **(E)** Summary plots of MBC2
743 and $CD23^+$ IL-$4R^{low}$ MBC frequency from IC and A4RA-treated epicutaneously sensitized mice.
744 **(F)** MFI of CD23 within OVA^+ (left) and OVA^- (right) MBCs from IC and A4RA-treated
745 epicutaneously sensitized mice. Pre-gated as $OVA^{+/-}$ B cells > $CD38^+$ $GL7^-$ > IgM^- IgD^-. **(G)**
746 Representative contour plots of MBC2s from human PBMCs 8 days following *in vitro* allergen
747 stimulation and treatment with IC or A4RA. Pre-gated as live > singlet > $CD3^-$ $CD14^-$ $CD16^-$
748 $CD19^+$ > IgD^- IgM^- > $CD38^{low\text{-}med}$. **(H)** Summary plots of human MBC2 frequency in **G**,
749 separated by CD27 expression. **(I)** MFI of CD23 within $CD27^{+/-}$ class-switched B cells from
750 human PBMCs 8 days following *in vitro* allergen stimulation and treatment with IC or A4RA.
751 Data represents 2-3 experiments with 5 mice per group and are presented as median ± min/max
752 (E, F) or 2 experiments (n = 3 blood donors) with each line representing a single donor (H, I). * p
753 < 0.05, ** p < 0.01, *** p < 0.001. Ab, antibody; Ag, antigen; LSC, lymphoid stromal cell.

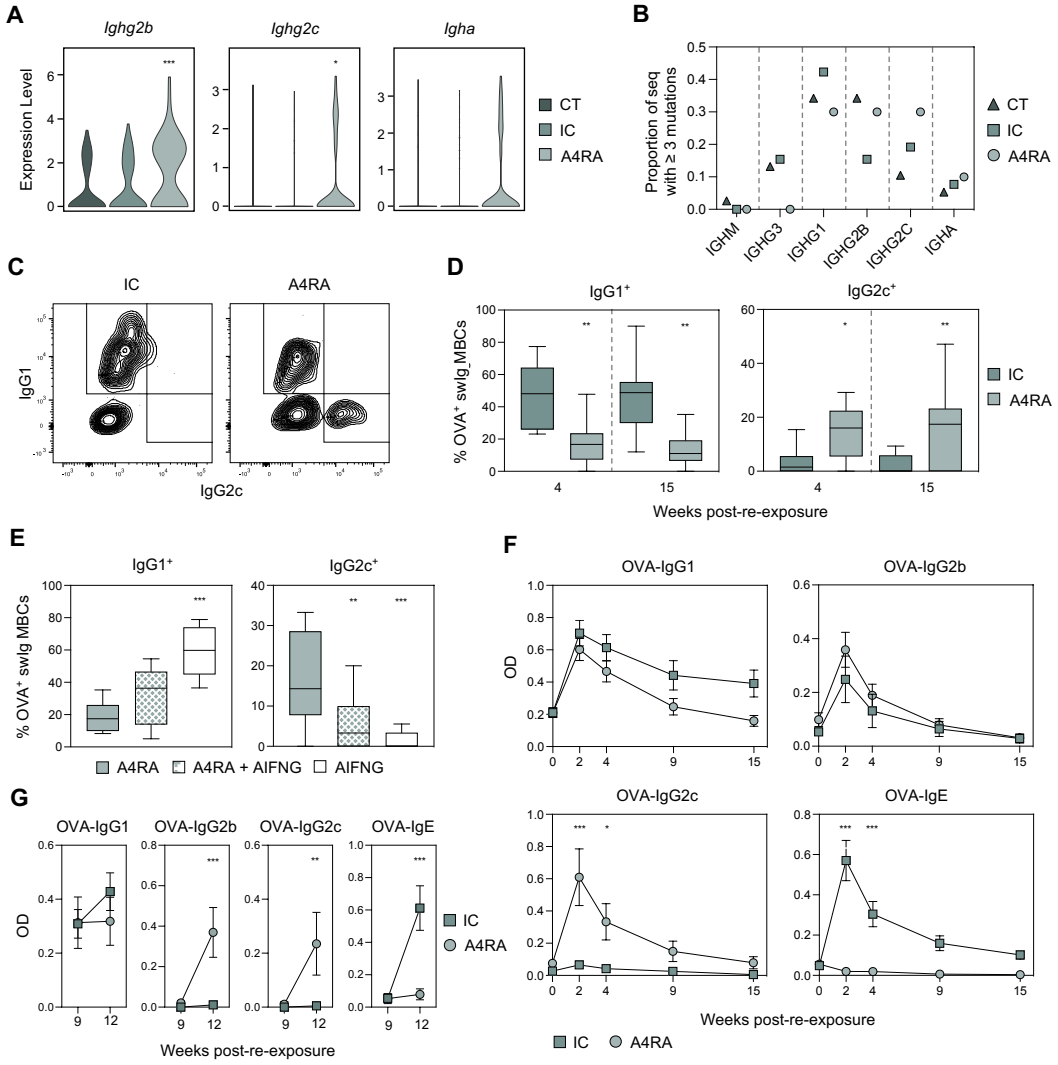
A
Ighg2b
Ighg2c
Igha
Expression Level
CT
IC
A4RA
B
Proportion of seq with ≥ 3 mutations
IGHM
IGHG3
IGHG1
IGHG2B
IGHG2C
IGHA
C
IC
A4RA
IgG1
IgG2c
D
IgG1+
IgG2c+
% OVA+ swIg MBCs
Weeks post-re-exposure
E
IgG1+
IgG2c+
% OVA+ swIg MBCs
A4RA
A4RA + AIFNG
AIFNG
F
OVA-IgG1
OVA-IgG2b
OVA-IgG2c
OVA-IgE
OD
Weeks post-re-exposure
IC
A4RA
G
OVA-IgG1
OVA-IgG2b
OVA-IgG2c
OVA-IgE
OD
Weeks post-re-exposure
IC
A4RA

754 **Fig. 3. Longitudinal analysis of Ag-specific B cell responses with absent IL-4 signaling. (A)**
755 Expression level of *Ighc* genes downstream of *Ighg1* from scRNA-seq analysis of B cells
756 isolated from spleens and inguinal LNs of CT-immunized mice and A4RA/IC-treated
757 epicutaneously sensitized mice. Gene expression is plotted for cells within the MBC cluster (Fig.
758 1B). **(B)** VDJ analysis of MBC cluster. Plot depicts the assigned *Ighc* gene in MBCs with ≥3
759 nucleotide mutations compared to the germline sequence. **(C)** Representative contour plots of
760 $IgG1^+$ and $IgG2c^+$ populations from inguinal LNs of IC/A4RA-treated epicutaneously sensitized
761 mice four weeks post-boost and antibody treatment. **(D)** IC/A4RA-treated mice were rested up to
762 15 weeks after re-exposures. $IgG1^+$ (left) and $IgG2c^+$ (right) MBC frequency are plotted at four
763 and 15 weeks post-boost. Pre-gated as OVA^+ B cells > $CD38^+$ $GL7^-$ > IgM^- IgD^-. **(E)**
764 Epicutaneously sensitized mice were treated with A4RA, AIFNG, or both at the time of
765 subcutaneous re-exposure. $IgG1^+$ (left) and $IgG2c^+$ (right) MBC frequency are plotted at four
766 weeks post-boost. Pre-gated as OVA^+ B cells > $CD38^+$ $GL7^-$ > IgM^- IgD^-. **(F)** OVA-specific
767 serum immunoglobulin profiles of IC/A4RA-treated mice at zero to 15 weeks post-boost. **(G)**
768 IC/A4RA-treated mice were rested for nine weeks to allow for clearance of OVA-specific IgG2c
769 and clearance of IC/A4RA blocking antibodies. Subsequently, mice received tertiary OVA
770 exposures and serum was collected at week 12. OVA-specific serum immunoglobulin profiles
771 are depicted before and after tertiary exposures. (C-G) Data represents 2 experiments with at
772 least 4 mice per group. Data are presented as mean ± SEM (F, G) or median ± min/max (D, E). *
773 $p < 0.05$, ** $p < 0.01$, *** $p < 0.001$. Seq, sequences; swIg, class-switched; AIFNG, anti-IFN-
774 γR1; OD, optical density.

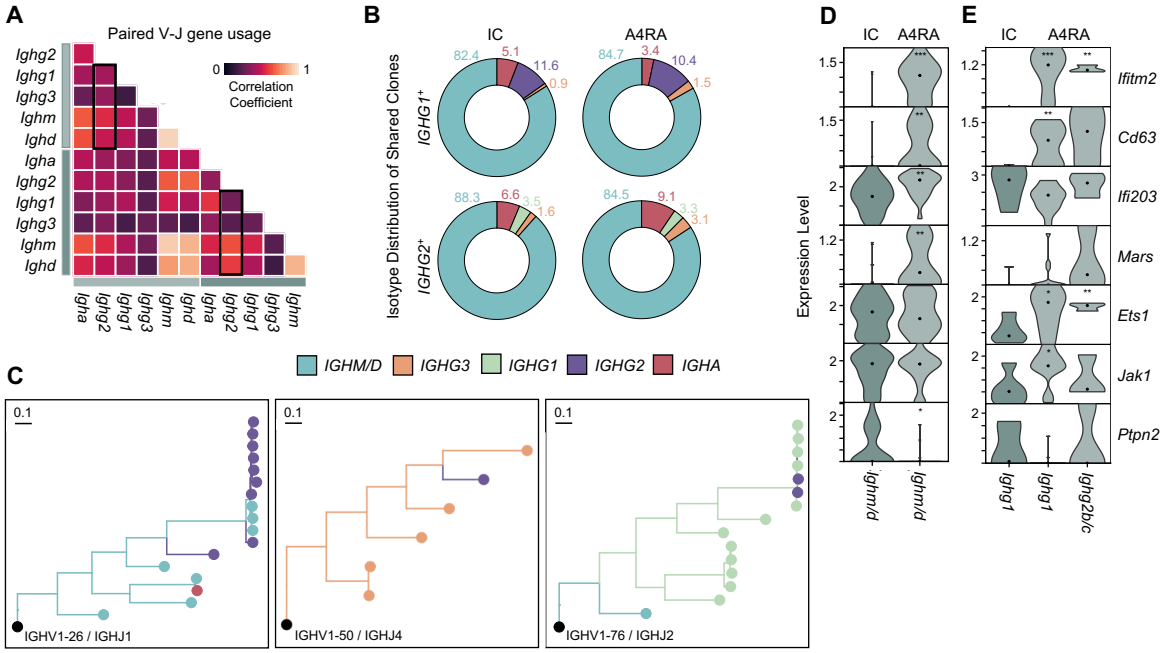
A
Paired V-J gene usage
Ighg2
Ighg1
Ighg3
Ighm
Ighd
Igha
Ighg2
Ighg1
Ighg3
Ighm
Ighd
Igha
Ighg2
Ighg1
Ighg3
Ighm
0
1
Correlation Coefficient
B
IC
A4RA
Isotype Distribution of Shared Clones
IGHG1+
IGHG2+
82.4
5.1
11.6
0.9
84.7
3.4
10.4
1.5
88.3
6.6
3.5
1.6
84.5
9.1
3.3
3.1
IGHM/D
IGHG3
IGHG1
IGHG2
IGHA
C
0.1
IGHV1-26 / IGHJ1
IGHV1-50 / IGHJ4
IGHV1-76 / IGHJ2
D
IC
A4RA
Expression Level
Ighm/d
Ighm/d
E
IC
A4RA
Ifitm2
Cd63
Ifi203
Mars
Ets1
Jak1
Ptpn2
Ighg1
Ighg1
Ighg2b/c

775 **Fig. 4. Clonal analysis of OVA-enriched B cells.** WT mice were epicutaneously sensitized with
776 OVA, then re-exposed s.c. to OVA in the presence of A4RA or IC. Four weeks post-boost,
777 spleens and inguinal LNs were collected. B cells from the OVA tetramer-enriched fraction were
778 sorted for bulk VDJ sequencing. **(A)** Correlation matrix of paired IGHV-IGHJ gene usage
779 between isotypes in IC and A4RA. Black boxes highlight the relationships between IgG2 and
780 upstream isotypes. **(B)** Circle plots showing the isotype distribution within clonal families
781 containing IGHG1 (top) and IGHG2 (bottom). **(C)** Representative clonal lineage trees containing
782 IGHG2 sequences and upstream isotypes (IGHM/D, IGHG3, and IGHG1) from A4RA-treated
783 mice. Scale indicates IGHV SHM frequency. **(D, E)** OVA-specific B cells were single-cell
784 sorted from epicutaneously sensitized mice at four weeks post-boost for Smart-Seq. $n = 40$ IC, n
785 $= 41$ A4RA. Expression level of select DEG are shown for unswitched (D) and IGHG1/2^{+} (E)
786 OVA-specific B cells. * $p < 0.05$, ** $p < 0.01$, *** $p < 0.001$.

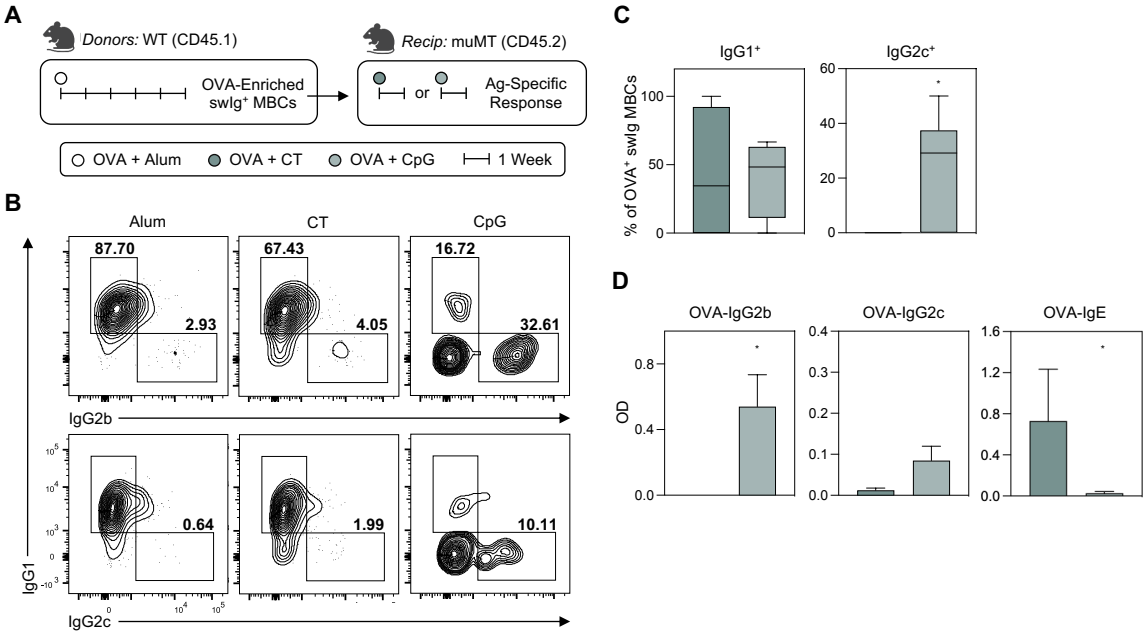
A
Donors: WT (CD45.1)
Recip: muMT (CD45.2)
OVA-Enriched swIg+ MBCs
or
Ag-Specific Response
OVA + Alum
OVA + CT
OVA + CpG
1 Week
B
Alum
CT
CpG
87.70
2.93
67.43
4.05
16.72
32.61
0.64
1.99
10.11
IgG2b
IgG1
IgG2c
C
IgG1+
IgG2c+
% of OVA+ swIg MBCs
D
OVA-IgG2b
OVA-IgG2c
OVA-IgE
OD

787 **Fig. 5. Boost with CpG produces IgG2 response from type 2-primed class-switched MBCs.**
788 **(A)** Adoptive transfer schematic. **(B)** WT mice were immunized with OVA + Alum, CT, or CpG.
789 Representative contour plots class-switched OVA^+ MBCs. Pre-gated as OVA^+ B cells > $CD38^+$
790 $GL7^-$ > IgM^- IgD^-. Numbers indicate the proportion of $IgG1^+$, $IgG2b^+$, and $IgG2c^+$ cells from the
791 parent class-switched MBC population. **(C)** OVA-enriched B cells were adoptively transferred
792 from WT OVA-Alum donor mice to naïve muMT mice and recipient were boosted with either
793 OVA + CT or OVA + CpG. Summary plots show OVA^+ $IgG1^+$ and OVA^+ $IgG2c^+$ B cell
794 frequency in recipient mice one week post-transfer and boost. **(D)** OVA-specific serum
795 immunoglobulin profiles in recipient mice one week post-transfer and boost. Data represents 2
796 experiments, each with 2-4 mice per group. Data are presented as median ± min/max (B) or
797 mean ± SEM (D). * $p < 0.05$.